

## Study of Nanocrystalline $\gamma$ -Al<sub>2</sub>O<sub>3</sub> Produced by High-Pressure Compaction

Tania M. H. Costa,<sup>†,‡</sup> Márcia R. Gallas,<sup>\*,†</sup> Edilson V. Benvenutti,<sup>‡</sup> and João A. H. da Jornada<sup>†</sup>

*Instituto de Física, UFRGS, Caixa Postal 15051, 91501-970 Porto Alegre (RS), Brazil, and  
Instituto de Química, UFRGS, Caixa Postal 15003, 91501-970 Porto Alegre (RS), Brazil*

*Received: September 21, 1998; In Final Form: February 10, 1999*

Using a high-pressure (HP) technique, samples of  $\gamma$ -Al<sub>2</sub>O<sub>3</sub> were obtained by compaction at 4.5 GPa, in a toroidal-type apparatus, at room temperature (RT) and at higher temperatures. Compaction at RT produced crack-free, translucent, and dense samples. An improvement of these properties was observed for samples compacted at higher temperatures up to 565 °C. The nanocrystalline structure of  $\gamma$ -Al<sub>2</sub>O<sub>3</sub> is retained, and the samples became transparent, showing high hardness (HV = 17 ± 1 GPa) and high density (95% of theoretical density). To understand the mechanisms of consolidation, a comparative analytical study by Fourier transform infrared spectroscopy (FTIR), thermogravimetric analysis (TGA), and X-ray diffraction (XRD) was conducted on the compacted  $\gamma$ -Al<sub>2</sub>O<sub>3</sub> samples and the original powder. An FTIR study was done using the KBr technique and a high-vacuum cell, where the samples were submitted to thermal treatments up to 450 °C. For samples compacted at RT, a reduction in the content of adsorbed water was observed, compared to the original powder. Also, the surface hydroxyl groups became bridged, promoting dehydroxylation reactions, which were confirmed by TGA technique. In the dehydroxylation region, a weight loss was observed, and the water was released only at temperatures above 300 °C. For samples compacted simultaneously with temperature, the FTIR and TGA results did not show water release up to 500 °C. The compaction at temperatures higher than 565 °C yielded the formation of an aluminum hydroxide (diaspore) and the phase transformation from  $\gamma$ - to  $\alpha$ -Al<sub>2</sub>O<sub>3</sub>. All these results support strongly the idea that the compaction at HP has caused the formation of a strong structure, with closed pores containing trapped water and hydroxylated internal surfaces, which confirms a proposed model for “cold-sintering”. At temperatures higher than 565 °C, this kind of structure is responsible for the formation of diaspore plus  $\alpha$ -Al<sub>2</sub>O<sub>3</sub>.

### Introduction

The  $\gamma$ -Al<sub>2</sub>O<sub>3</sub> is one of the transition aluminas widely used in technology, in the form of powder or thin film, as adsorbents, catalysts or catalysts carriers, coatings, and soft abrasives because of their fine particle size, high surface area, and catalytic activity. The possibility of obtaining  $\gamma$ -Al<sub>2</sub>O<sub>3</sub> nanocrystalline bulk samples from nanosize particles has been investigated over the last few years<sup>1–3</sup> in order to produce a new material with interesting specific properties. It was not possible to prepare this material in bulk some years ago due to phase transformation sequences that occur during the conventional sintering process at ambient pressure:  $\gamma$ (750 °C)  $\rightarrow$   $\delta$ (900 °C)  $\rightarrow$   $\theta$ (> 1000 °C)  $\rightarrow$   $\alpha$ . The use of the HP technique provides the means to overcome this difficulty. Gallas et al.<sup>3</sup> reported the fabrication of transparent and hard  $\gamma$ -Al<sub>2</sub>O<sub>3</sub> samples (about 0.2 mm of diameter) using a diamond anvil HP cell (DAC) to compact a nanosize powder at pressures up to 3 GPa, followed by pressureless heat treatment at 800 °C. Recently, using another HP technique with a nearly hydrostatic pressure transmitting medium at pressures up to 5.6 GPa and RT, it was possible to produce larger (3.0 mm of diameter)  $\gamma$ -Al<sub>2</sub>O<sub>3</sub> samples, translucent and with high density, indicating a process of “cold-sintering”. In this paper, the results of density measurements vs applied pressure fit a model based mostly on a mechanism

of plastic deformation.<sup>4</sup> Costa et al.<sup>5</sup> studied this process for SiO<sub>2</sub> gel powders treated at HP and RT. They proposed a model for the “cold-sintering” process based on condensation reactions of silanol groups at the surface of the nanoparticles to form siloxane bonds between the particles and water, resulting in a stiff body with closed nanopores contained trapped water. It was clear from this model that the adsorbed water plays an important role in the mechanism of consolidation of this kind of powder, which is covered by OH groups.

A small number of works involving compaction studies of  $\gamma$ -Al<sub>2</sub>O<sub>3</sub> at HP and high temperature (HT) are found in the literature. Mishra et al.<sup>1</sup> studied the HP sintering of  $\gamma$ -Al<sub>2</sub>O<sub>3</sub> samples over the temperature range 650–1050 °C and pressures of 1 GPa; however, they did not specify the physical appearance of the compacts and did not study the microscopic mechanism involved in the consolidation process.

Several techniques based on FTIR spectroscopy have been widely used to characterize  $\gamma$ -Al<sub>2</sub>O<sub>3</sub> films and powders made by different methods<sup>8,9</sup> and to obtain a microscope understanding of the processes involved in these systems.<sup>8–12</sup> The FTIR spectrum of  $\gamma$ -Al<sub>2</sub>O<sub>3</sub> is well-known, and its principal feature is a broad band between 950 and 500 cm<sup>−1</sup>, ascribed to Al–O stretching. The surface of  $\gamma$ -Al<sub>2</sub>O<sub>3</sub> is covered by OH groups that cause water adsorption, and the band due to these species is between 3800 and 3000 cm<sup>−1</sup>, centered at 3460 cm<sup>−1</sup>. This band is ascribed to OH stretching of the adsorbed water, to the bridged hydroxyl group with molecular water or with other OH groups, and to isolated OH groups.<sup>10</sup> The study of all these bands

\* Corresponding author. Phone: +55-51 316 6542. Fax: +55-51 319 1762. E-mail: marcia@if.ufrgs.br.

<sup>†</sup> Instituto de Física.

<sup>‡</sup> Instituto de Química.

enables the acquisition of valuable information about the coverage of the  $\gamma$ -Al<sub>2</sub>O<sub>3</sub> surface.

In this work, the effect of thermal treatments at HP (4.5 GPa), from RT up to 870 °C, in  $\gamma$ -Al<sub>2</sub>O<sub>3</sub> nanosize powders was studied through a comparative analytical study by FTIR, TGA, and XRD, in the obtained samples and the original powder. The goals of this study are to obtain a new material, with improved optical and mechanical properties; to identify the sequence of phases produced by this process up to the onset of the  $\alpha$  phase, and to understand the microscopic mechanism involved in the compaction process promoted by HP, especially with regard to the role of adsorbed water in the system.

## Experimental Section

The  $\gamma$ -Al<sub>2</sub>O<sub>3</sub> nanosize powder used was a commercially available material, Aluminum Oxide C, supplied by Degussa AG, Frankfurt, Germany. It has an average primary particle size of 13 nm and a purity of 99.6%, according to the technical specifications.<sup>16</sup> The  $\gamma$ -Al<sub>2</sub>O<sub>3</sub> phase has a cubic spinel-like structure (*Fd3m*), which consists of 32 atoms of oxygen, 21 1/3 atoms of Al, and 2 2/3 vacancies per unit cube, with an edge of 7.9 Å. This corresponds to a volume of 46.2 Å<sup>3</sup> per molecule,<sup>7</sup> yielding a theoretical density of 3.66 g/cm<sup>3</sup>. In several works, the adopted value was 3.2 g/cm<sup>3</sup>, which implies considerable errors in the calculations of relative density.

High-pressure experiments were done at RT and at higher temperatures (HT) up to 870 °C. For the HP experiments at RT, the  $\gamma$ -Al<sub>2</sub>O<sub>3</sub> powder was initially precompacted in a piston-cylinder-type die to approximately 0.1 GPa. The volume of the precompacted sample was about 100 mm<sup>3</sup> (diameter  $\approx$  5 mm, height  $\approx$  5 mm). Samples were then placed in a Pb container that acts as a nearly hydrostatic pressure-transmitting medium and compacted at 4.5 GPa.<sup>4</sup> For the experiments at higher temperature, the precompacted samples had a volume of about 50 mm<sup>3</sup> (diameter  $\approx$  4 mm, height  $\approx$  4 mm). These samples were placed in a boron nitride (hBN) container surrounded by a graphite heater. First, the samples were compacted at 4.5 GPa at RT, and then the temperature was raised to the desirable value, up to 870 °C, and was maintained for 10 min. The RT and HT containers were assembled in a toroidal-type chamber, and a detailed description of this HP method is given elsewhere.<sup>17</sup>

Compacted samples were investigated by optical microscopy to detect cracks and to evaluate their optical transparency. Vickers microhardness measurements were performed using a Shimadzu microindenter with typical loads of 100 g and a dwell time of 15 s. The samples were previously polished with silicon carbide sandpaper grade 1000 and diamond paste. Archimede's method was used to measure density. X-ray diffraction patterns were obtained with a Siemens diffractometer D500.

A comparative study was made with three kind of samples: original powder, compacted samples at RT, and compacted samples at HT, using FTIR and TGA. In the transmission FTIR spectroscopy, analyses were done using the KBr technique and a high-vacuum cell. For KBr analyses, samples were crushed in an agate mortar and sieved to 400 mesh, mixing thoroughly with powdered KBr to 1.5 wt % and pressed to form a transparent pellet. The KBr was previously dried for 4 h at 150 °C to eliminate water. For the vacuum cell, a self-supporting disk of the original alumina powder with an area of ca. 5 cm<sup>2</sup> and mass of ca. 40 mg, was prepared. For the compacted samples at RT and HT, thin polished slices with a thickness between 0.09 and 0.3 mm and a diameter of 3 mm, placed in a stainless steel support, were used. The vacuum cell, described elsewhere,<sup>18</sup> was connected to a greaseless vacuum line, and

the sample was heated for 1 h at 100, 200, 300, 400, and 450 °C, under dynamic vacuum of 10<sup>-3</sup> Pa. FTIR spectra were obtained at RT under vacuum, after each heat treatment, without exposing the sample to air. The equipment used in this series of measurements was a Bomem FTIR spectrometer (model MB-102) with a resolution of 4 cm<sup>-1</sup> and a maximum of 500 scans.

Thermogravimetric analysis was done on a Perkin-Elmer thermogravimetric analyzer. The  $\gamma$ -Al<sub>2</sub>O<sub>3</sub> original powder was analyzed as-prepared. For the compacted samples obtained by the HP treatment at RT and HT, the analyses was made in small pieces of the slices of the same kind used in the FTIR measurements. The samples were heated from RT to 900 °C at a rate of 20 °C/min. in a dry nitrogen atmosphere.

Surface area values were obtained with a Micromeritics 2010 system using a multipoint BET method and powdered samples.

## Results and Discussion

**Compaction at Room Temperature.**  $\gamma$ -Al<sub>2</sub>O<sub>3</sub> samples obtained in the HP experiments were crack-free, optically translucent, and dense. Their densities were  $2.95 \pm 0.04$  g/cm<sup>3</sup>, corresponding to 80% of full density (estimated at 3.66 g/cm<sup>3</sup>),<sup>7,19</sup> which is very high, considering that compaction was performed at RT. An average Vickers microhardness of  $4.5 \pm 0.2$  GPa was measured, indicating a very well consolidated body, and the values of bulk density indicate densification. These characteristics were already described in a previous paper.<sup>4</sup> The BET surface area for the original samples was  $98.8 \pm 0.6$  m<sup>2</sup>/g, and for the compacted samples it was  $78.1 \pm 0.1$  m<sup>2</sup>/g, with an average pore diameter of  $11.7 \pm 0.1$  nm and  $5.5 \pm 0.1$  nm, respectively. The BJH adsorption cumulative volume of pores between 1.7 and 300 nm was 0.181 cm<sup>3</sup>/g for the original samples and 0.088 cm<sup>3</sup>/g for the compacted samples, indicating a reduction in porosity and pore diameter. The observed decrease in surface area is not very impressive. However, it should be taken into account that the samples were comminuted, introducing microcracks in the small particles.

Typical FTIR absorption spectra for  $\gamma$ -Al<sub>2</sub>O<sub>3</sub> taken at RT using the KBr technique are shown in Figure 1. The spectrum for the original powder is shown in Figure 1a. The large band between 1000 and 400 cm<sup>-1</sup> is a characteristic absorption band of transition aluminas. According to literature,<sup>8</sup> it is attributed to stretching vibration of the Al—O—Al bond and the broadening of this band is due to the distribution of vacancies among the octahedral and tetrahedral sites, leading to a spreading out of the Al—O vibrational frequencies. More specific studies were made by Ying<sup>9</sup> using photoacoustic FTIR in alumina nanoclusters and nanostructured samples compacted at 1 GPa, as well as the  $\gamma$ -Al<sub>2</sub>O<sub>3</sub> powder from Degussa. Their spectra showed the broad alumina band for all samples, and it was deconvoluted in three components: component 1 represents the surface phonon mode of alumina; component 2 and component 3 correspond to Al—O—Al stretching in the tetrahedron and octahedron sites, respectively.

In addition to alumina bands, there are bands due to chemisorbed and adsorbed species at the surface. The very large band centered at 3460 cm<sup>-1</sup> results from a superposition of vibration bands of bonded hydroxyl groups, isolated OH groups, and stretching vibrations of adsorbed water molecules. At RT, all these bands are superimposed and the resolution is difficult.<sup>10,11</sup> The band at 1630 cm<sup>-1</sup> is due to bending of molecular water. The two small bands between 1500 and 1400 cm<sup>-1</sup> are attributed to chemically adsorbed impurities of CO<sub>2</sub>, CO, CO<sub>3</sub><sup>2-</sup>, or HCO<sub>3</sub><sup>-</sup> that are very difficult to remove, even at temperatures of 800 °C.<sup>9</sup> The band between 2860 and 2960 cm<sup>-1</sup> corresponds to H—C stretching.

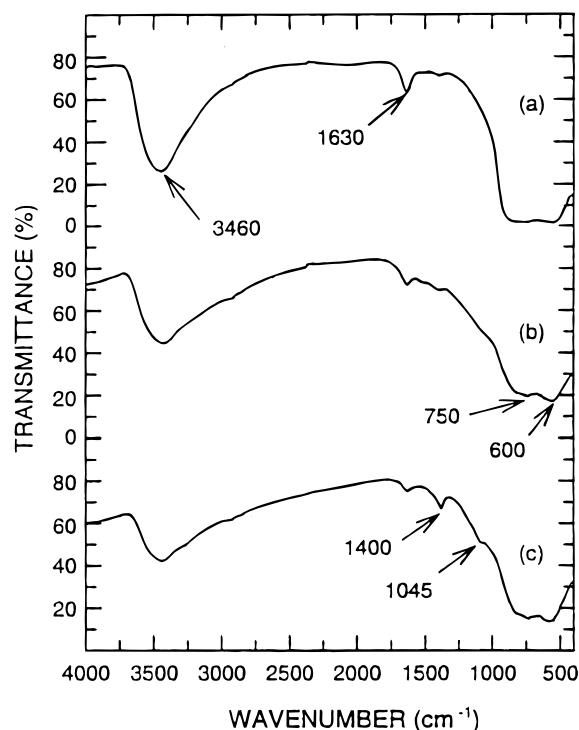


**Figure 1.** Typical FTIR spectra of  $\gamma$ - $\text{Al}_2\text{O}_3$  samples using the KBr technique: (a) original powder at ambient pressure; (b) compacted sample at  $P = 4.5$  GPa and RT; (c) compacted sample at  $P = 4.5$  GPa and 500 °C.

Figure 1b shows a spectrum for  $\gamma$ - $\text{Al}_2\text{O}_3$  compacted at 4.5 GPa at RT. There are some differences between parts a and b of Figure 1. The bulk alumina bands showed a better definition due to the formation of a more ordered structure, caused by the HP treatment, and two peaks can be observed: one ca. 750  $\text{cm}^{-1}$  and another ca. 600  $\text{cm}^{-1}$ . The band at 600  $\text{cm}^{-1}$  is slightly more intense than the other, and according to Ying's studies,<sup>9</sup> it indicates a higher occupation of the octahedral sites. These sites have a higher coordination and their occupation will be favored by HP treatment. The same effect was observed by Baraton and Quintard,<sup>8</sup> in alumina samples treated at 950 °C for 5 h. Also, there is a reduction on the width of the alumina bulk band, which enables the observation of a shoulder at ca. 1045  $\text{cm}^{-1}$ , assigned to the Al–O stretching of the surface component. Concerning the surface and impurity bands, another difference is observed. There is a considerable area reduction for the very large band centered at 3460  $\text{cm}^{-1}$  and for the 1630  $\text{cm}^{-1}$  band, which was used to make a semiquantitative determination of water content of the samples. It can be seen in Figure 1b that the area of the 1630  $\text{cm}^{-1}$  band decreases 33% after HP compaction. Therefore, it can be estimated that the water content is reduced by the same factor. The bands between 1500 and 1400  $\text{cm}^{-1}$  are still observed, indicating that the  $\text{CO}_2$  molecules chemically adsorbed were not eliminated by the HP treatment.

Figure 1c shows the spectrum of the samples compacted at 4.5 GPa and 500 °C and will be discussed in the next section.

Figure 2 shows the FTIR absorption spectra obtained in the vacuum cell after heat treatment at different temperatures in the range between 4000 and 2000  $\text{cm}^{-1}$  for original  $\gamma$ - $\text{Al}_2\text{O}_3$  powders. Figure 2a shows the spectrum obtained without any previous treatment, where the broad band from 3800 to 2700  $\text{cm}^{-1}$  is ascribed to OH stretching of various species explained previously. This band is superimposed on the stretching C–H band of adsorbed impurities on the original sample. Although

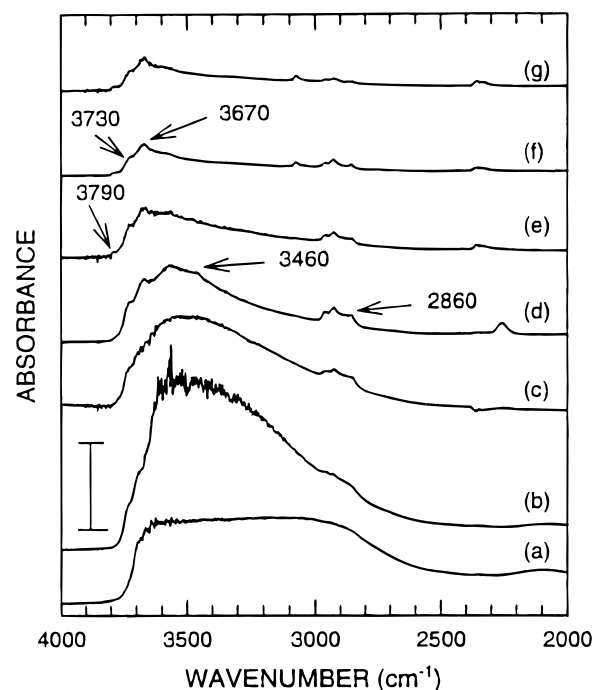


**Figure 2.** FTIR transmission spectra of original  $\gamma$ - $\text{Al}_2\text{O}_3$  powder obtained in a vacuum cell after treatment at different temperatures: (a) RT and ambient pressure; (b)–(g) obtained in a vacuum at (b) RT, (c) 100, (d) 200, (e) 300, (f) 400, and (g) 450 °C. The bar value is 1 in absorbance units.

the pellet used to take the spectrum was as thin as possible, it showed saturation, due to the high content of adsorbed water. In parts b, c, and d of Figure 2, respectively, at RT, 100 °C, and 200 °C, a reduction of the 3800–2700  $\text{cm}^{-1}$  bandwidth and intensity was observed, which is expected for this kind of powder.<sup>10–12</sup> It is caused by adsorbed water elimination and dehydroxylation reaction of bonded groups. In the spectrum of Figure 2d, some peaks could be observed at 3790, 3730, 3670 (maximum of absorption), and 3460  $\text{cm}^{-1}$ . The first three peaks are attributed to isolated OH groups, which are characteristics of aluminas heat treated at moderate temperatures, being very difficult to resolve.<sup>11,13,20</sup> The peak at 3460  $\text{cm}^{-1}$  is assigned to OH stretching of bonded groups, and after heat treatment at 300 °C (Figure 2e), it is eliminated. At higher temperatures (parts f and g of Figure 2), only the three peaks related to the isolated OH groups remain. There is a great controversy in the literature about the attribution of these peaks. In this work, the approach of Knözinger et al.<sup>10</sup> was adopted, whose configurations are represented in Figure 3. The OH groups of Ia and Ib types (3790  $\text{cm}^{-1}$ ) can rotate and orient themselves to make interactions with adjacent groups. The IIa and IIb types (3730  $\text{cm}^{-1}$ ) are unfavorable to form bridges with another fixed groups, and the III type (3670  $\text{cm}^{-1}$ ) is totally hampered to make interactions. The peaks of the II and III types are not influenced by the dehydroxylation process, maintaining their intensities.<sup>10</sup> The profile of dehydroxylation shown in Figure 2 agrees with the results found in the literature.

Figure 4 shows the FTIR absorption spectra, in the range between 4000 and 2000  $\text{cm}^{-1}$ , of thin slices of  $\gamma$ - $\text{Al}_2\text{O}_3$  samples compacted at RT, obtained in the vacuum cell after heat treatment at different temperatures. Figure 4a shows the spectrum obtained without any previous treatment, where a broad band from 3800 to 2700  $\text{cm}^{-1}$  is observed. This band has the same attributions already described in the case of Figure 2a, although now, it is broader. This broadening is explained by the saturation of the spectra, caused by the water retained in

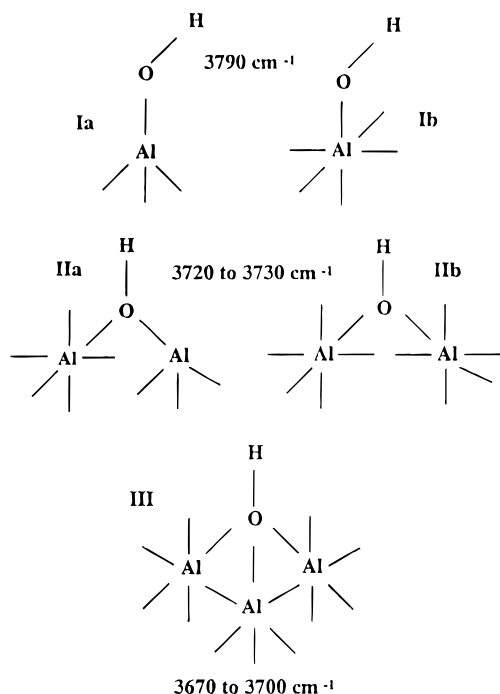


**Figure 3.** Configurations proposed by Knözinger et al.<sup>10</sup> to represent the different kinds of surface OH groups of transition aluminas.

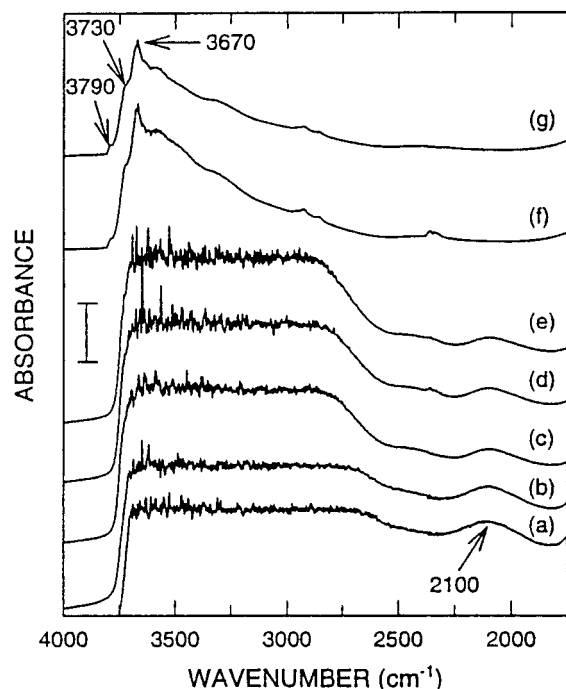


**Figure 4.** FTIR absorption spectra of thin slices of  $\gamma$ - $\text{Al}_2\text{O}_3$  samples obtained in a vacuum cell after treatment at different temperatures. (a) RT and ambient pressure; (b)–(g) obtained in a vacuum at (b) RT, (c) 100, (d) 200, (e) 300, (f) 400, and (g) 450 °C. The bar value is 1 in absorbance units.

the sample by HP treatment (Figure 1b), and it occurs even when very thin slices were used (90  $\mu\text{m}$ ). The existence of the band at 2100  $\text{cm}^{-1}$  confirm this fact, because this band appears only when there is a great quantity of water. After the heat treatment at 100 °C (Figure 4c), the large band between 3800 and 2700  $\text{cm}^{-1}$  became narrow, and this profile persists up to 300 °C (Figure 4e). Only after the heat treatment at 400 °C (Figure 4f) does this profile change considerably, because the band due to OH bonded groups and water disappeared. The

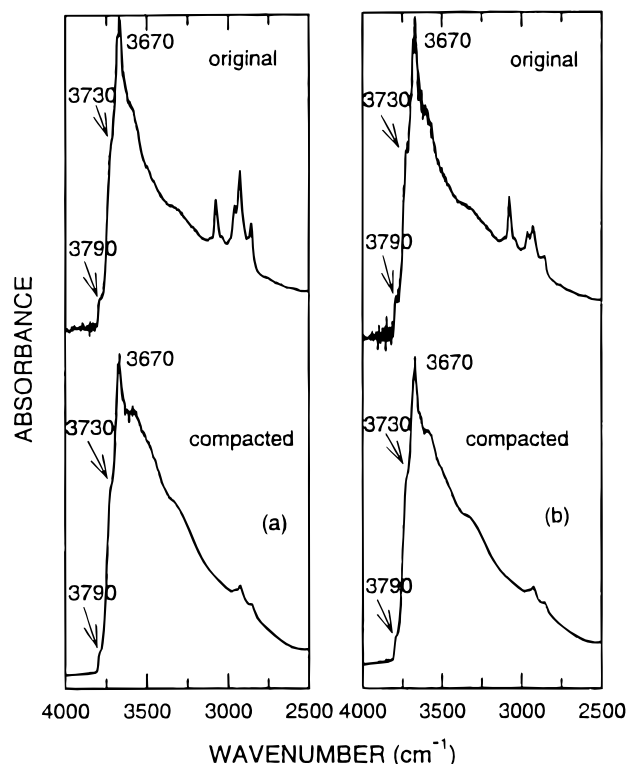


**Figure 5.** FTIR normalized spectra of  $\gamma$ - $\text{Al}_2\text{O}_3$  samples obtained in a vacuum cell after thermal treatment at (a) 400 °C and (b) 450 °C.

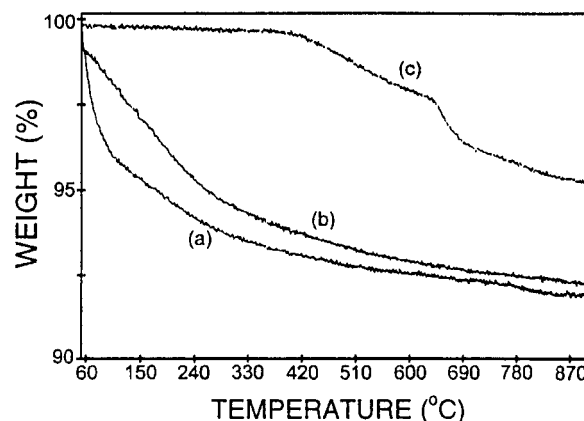


**Figure 6.** Thermogravimetric curves for  $\gamma$ - $\text{Al}_2\text{O}_3$  samples obtained in a nitrogen atmosphere up to 900 °C at a heating rate of 20 °C/min: (a) original powder; (b) compacted sample at  $P = 4.5$  GPa and RT; (c) compacted sample at  $P = 4.5$  GPa and 500 °C.

same shape and profile of the original sample (parts f and g of Figures 2) is maintained at 450 °C. For a detailed comparison, Figure 5 exhibits a normalized spectra for Figures 2f,g and 4f,g in the region between 4000 and 2500  $\text{cm}^{-1}$ . A broadening in the low-frequency region for the compacted sample was observed, indicating the formation of hydrogen bonds between surface groups. However, the isolated OH bands persist with the same relative intensities, because the formation of H bonds (3730  $\text{cm}^{-1}$ ) is restricted or even impossible (3670  $\text{cm}^{-1}$ ), according to the configurations showed in Figure 3.

Figure 6 shows typical thermograms obtained for the original  $\gamma$ - $\text{Al}_2\text{O}_3$  powders (part a), for slices of compacted samples at RT (part b), and for slices of compacted samples at HT (part c). Uncertainties in TGA measurements were 0.2% for temperature and 0.5% for weight. Thermogram a presents a total weight loss of 8.8%, and 60% of this loss occurred from RT to 150 °C, which is ascribed to elimination of adsorbed water. The



**TABLE 1: Physical Properties of  $\gamma$ -Al<sub>2</sub>O<sub>3</sub> Samples Processed at 4.5 GPa, during 10 Min and Temperatures between 465 and 870 °C**

sample	temp (°C)	phases present	optical appearance	physical appearance	microhardness (GPa)	density (g/cm <sup>3</sup> )
1	465	$\gamma$	transparent	brittle		
2	514	$\gamma$	transparent	crack-free	17.7 ± 0.7	3.43 ± 0.01
2* <sup>a</sup>	515	$\gamma$	opaque	brittle		
3	565	$\gamma$	transparent	crack-free	16.7 ± 0.6	3.49 ± 0.01
4	562	$\gamma$	transparent	crack-free	17 ± 1	3.44 ± 0.01
5	577	$\gamma + \alpha + D^b$	dark/transparent	brittle		
6	594	$\gamma + \alpha + D$	black/transparent	brittle		
7	755	$\alpha + D + B^c$	dark gray	brittle		
8	870	$\alpha + B$	dark gray	brittle		

<sup>a</sup> \* denotes sample was previously dried at 500 °C for 1 h. <sup>b</sup> Diaspore. <sup>c</sup> Aluminum borate.

remained 40% of the total weight loss is eliminated between 150 and 900 °C, due to dehydroxylation of the surface and elimination of adsorbed organic impurities. In thermogram b we observe a total weight loss of 7.8%, and from RT up to 150 °C, only 37% of this value is lost. In this range of temperature, the weight loss of the compacted sample at RT is lower than that of the original powder, which can be explained by the reduction of adsorbed water of the compacted samples and by the retention of the water in the sample. These facts were observed in the FTIR spectrum of Figure 1b and mainly in the spectra of Figure 4, where the corresponding bands of adsorbed water and OH bonded groups remain up to 400 °C. Comparing the total weight loss of the original powders and the compacted samples, we notice very similar values (8.8 and 7.8%, respectively). This fact can be explained as follows. In the range from 150 to 420 °C, the weight loss of the original powder is 1.1% and that for the compacted sample is 1.9%. In this range of temperature occurs the dehydroxylation reaction, and these reactions are facilitated by HP treatment that promotes the formation of H bridges between OH groups. This fact increases the weight loss in this range of temperature causing almost the same total weight loss for both samples. This point was fully discussed in a previous paper about compaction of silica powders.<sup>5</sup> Thermogram c will be discussed in the next section.

The data from Figure 4 and from the TGA (Figure 6) show a “delay” to release water of compacted samples, indicating that water is retained in closed pores. Total elimination of adsorbed water occurs only above 300 °C, after a rupture of these closed pores caused by the internal pressure of water vapor, which becomes possible at higher temperatures. This indicates the existence of a strong closed-pore structure formed during the HP treatment.

All FTIR and TGA results can be qualitatively explained by a cold-sintering process promoted by HP at RT, occurring through dehydroxylation reaction of surfaces OH groups, which forms Al—O—Al bonds. The “cold-sintering” mechanism was proposed recently for SiO<sub>2</sub> obtained from the sol—gel method and compacted at HP and RT. This model is based on the reverse of what occurs in the slow fracture model for SiO<sub>2</sub>, proposed by Freiman and Michalske,<sup>21</sup> being discussed in detail in ref 5. Although there are differences between the structure of SiO<sub>2</sub> (amorphous) and  $\gamma$ -Al<sub>2</sub>O<sub>3</sub> (crystalline) and the synthesis method, both powders have the surface covered by OH groups and adsorbed water, which enable the dehydroxylation reaction and, consequently, the cold-sintering process at high pressure.

**Compaction at Higher Temperature.** The HP experiments (4.5 GPa) at higher temperatures (up to 870 °C, during 10 min) and the physical properties of the samples are summarized in Table 1. The samples processed up to 513 °C maintain the  $\gamma$  phase and are transparent, but they are not well consolidated, showing cracks and separate fragments. We interpreted this as

being caused by the HP medium that is not hydrostatic enough compared to the configuration used at RT experiments. However, from 513 to 565 °C, we obtain very good samples with the  $\gamma$ -Al<sub>2</sub>O<sub>3</sub> phase retained. These samples are transparent, crack-free, and dense, with values for density of 3.49 ± 0.01 g/cm<sup>3</sup> (95% of theoretical density) and a Vickers microhardness of 17 ± 0.7 GPa (100 g load). These values are much greater than those reported in the literature by Mishra et al.,<sup>1</sup> on samples compacted at 1 GPa and 750 °C during 15 min, where they obtained a density of 3.3 g/cm<sup>3</sup> and a Vickers microhardness of 7.3 ± 0.2 GPa.

According to Table 1, the samples that are compacted at temperatures higher than 565 °C are brittle and dark, which is a consequence of a phase mixture. Dark aluminas are mentioned in the literature, and this characteristic is attributed to oxygen deficient transition phases or to reduced CO<sub>2</sub> adsorbed on the original sample. The  $\gamma$  phase is maintained simultaneously with two other phases,  $\alpha$  and D (diaspore, an aluminum monohydroxide).<sup>6</sup> Above 600 °C, the  $\gamma$  phase disappeared, the  $\alpha$  phase and diaspore remained, and a new phase is formed due to the reaction with the hBN container. This phase is an aluminum borate and was called B.<sup>22</sup> At 871 °C, only the  $\alpha$  and B phases are present.

Figure 7 shows the XRD patterns for the original sample and for samples compacted at 4.5 GPa and temperatures between 562 and 871 °C. In parts a and b of Figure 7, typical patterns of  $\gamma$  alumina are observed, corresponding to ASTM card 10-425 and 4-877, based in a cubic spinel-like structure. These patterns present broad line widths, a characteristic of nanocrystalline materials. A small increase in the line width (~20%) is observed for sintered samples, which could be related to internal stress due to HP compaction. This same effect was observed previously.<sup>4</sup> This result corroborates that a significant grain growth did not occur and the nanocrystallite size is maintained. Figure 7c shows the characteristic peaks of three phases:  $\gamma$  phase,  $\alpha$  phase, and diaspore (D). At 755 °C (Figure 7d), the  $\alpha$  phase is dominant, a small quantity of diaspore is retained, and characteristic peaks of hexagonal boron nitride (BN) are also seen. This impurity is a residue which remained at the sample surface, coming from the hBN container used in the high-pressure/high-temperature (HP/HT) experiments. Figure 7e shows mainly  $\alpha$  phase, with very small quantities of hBN and an aluminum borate (B).

The presence of diaspore, detected at 577 °C, shows the transformation of an oxide in a hydroxide. It can occur at HP, and it is caused by water retention in the samples, revealed by the FTIR spectra (Figure 1) and TGA (Figure 6). The presence of trapped water yields the necessary conditions to transform  $\gamma$  alumina into diaspore.<sup>23,24</sup> Subsequently, diaspore transforms to  $\alpha$  phase at higher temperatures. The crystalline structure of these two phases is similar (hcp); therefore, the transformation

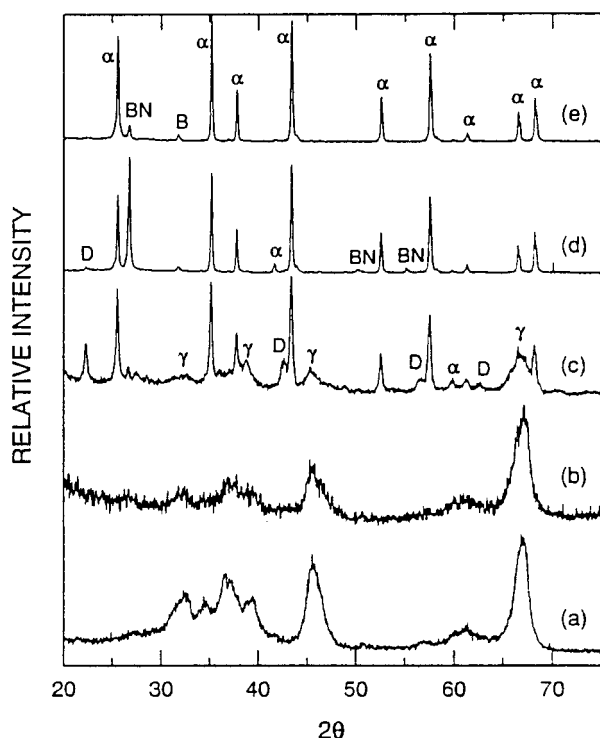


**Figure 7.** X-ray powder diffraction pattern of  $\gamma$ - $\text{Al}_2\text{O}_3$ , (a) original powder, and samples compacted at 4.5 GPa at (b) 562, (c) 577, (d) 755, and (e) 871 °C. The peaks are identified as  $\alpha$  for  $\alpha$  phase,  $\gamma$  for the  $\gamma$  phase, B for aluminum borate, BN for boron nitride, and D for diaspore.

from one to another is topotactic, with  $\alpha$  alumina being the only product of the decomposition of diaspore.

The aluminum borate peak (B) shown in Figure 7e appeared due to the reaction of the hBN container, in the presence of water, with  $\text{Al}_2\text{O}_3$ , forming  $9\text{Al}_2\text{O}_3 \cdot 2\text{B}_2\text{O}_3$ . This borate was synthesized for the first time, under HP, by Capponi et al.<sup>25</sup> It is eliminated at temperatures higher than 1214 °C.

To study the effects of the presence of water in  $\gamma$  alumina samples, some of them were dried and others were moistened, just before the HP/HT compaction. The sample marked in Table 1 as 2\* was dried at 500 °C during 1 h before the HP/HT compaction at 515 °C. Although the  $\gamma$ - $\text{Al}_2\text{O}_3$  is the only phase present, the sample became brittle and opaque, and it was not possible to measure its density and hardness, showing that the water plays an important role in the process of compaction. According to previous works,<sup>3,26</sup> it is very difficult to achieve high density in compacts from nanosize particles, and it was proposed that the use of suitable lubricant can improve their packing properties. This better packing promotes the sintering process through the condensation reaction of OH groups, which is the cold-sintering mechanism already discussed.<sup>5</sup>

Figure 8 shows the diffraction patterns for samples compacted near 600 °C. In Figure 8a, 20% in weight of water was added to the sample, and a significant increase of the diaspore peaks was observed, compared to the normal samples (Figure 8b). For samples previously dried at 500 °C for 1 h (Figure 8c), there is still formation of diaspore, indicating that the water content and the OH groups that remain in the particle surface promote this kind of transformation.

Regarding the water absorption and retention in experiments at HP/HT, the FTIR spectra and TGA thermograms are very useful. Figure 1c shows a KBr spectrum of a typical sample compacted at 4.5 GPa and temperature of 500 °C. This spectrum is very similar to that in Figure 1b (sample compacted at RT),

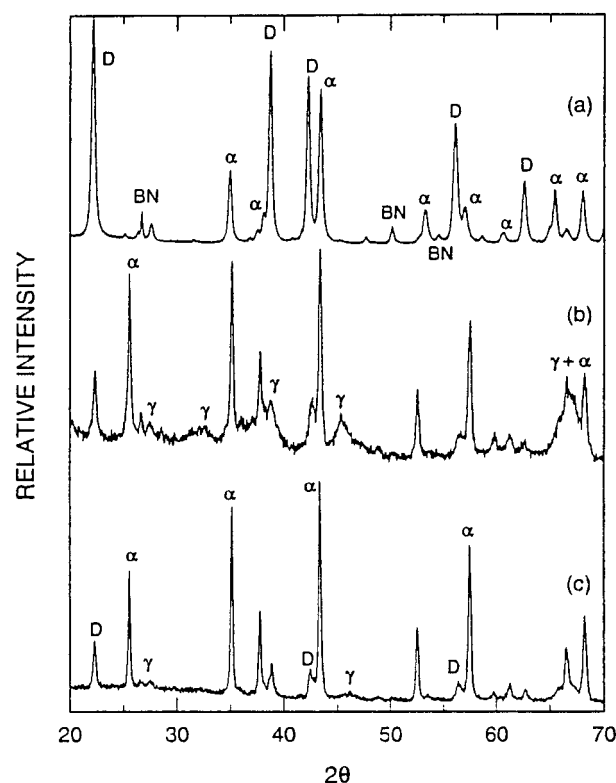


**Figure 8.** XRD pattern of  $\gamma$ - $\text{Al}_2\text{O}_3$  samples compacted at 4.5 GPa and at a temperature of approximately 600 °C: (a) original powder with 20% in weight of water; (b) original powder; (c) original powder dried at 500 °C for 1 h. The peaks are identified as  $\alpha$  for  $\alpha$  phase,  $\gamma$  for the  $\gamma$  phase, BN for boron nitride, and D for diaspore.

showing the same characteristics previously discussed. However, an area reduction of 44.5% is observed for the  $1630\text{ cm}^{-1}$  band, compared to the sample compacted at RT. It indicates a reduction of the adsorbed water on the surface or trapped in pores. This band reduction can be caused either by evaporation or by an hydroxylation on the surface of internal pores during the HP/HT compaction. Additionally, in Figure 1c, the presence of species generated by the chemical adsorption of  $\text{CO}_2$  in air ( $1400\text{ cm}^{-1}$ ) can be detected.

Figure 9 shows FTIR absorption spectra obtained in the vacuum cell after heat treatment at different temperatures for samples compacted at 4.5 GPa and 562 °C. In this figure, all the spectra show the same profile. A broad band between  $3750$  and  $2800\text{ cm}^{-1}$ , attributed to OH groups, and the band of water combination at  $2100\text{ cm}^{-1}$  are present. For the spectra after heat treatment between 300 and 400 °C (Figures 9d–f), a small reduction on the width of the OH band and on the intensity of the  $2100\text{ cm}^{-1}$  band is observed. However, the general profile of the spectra is not modified. The adsorbed water remains trapped in closed pores and is not liberated even after heat treatment in a vacuum at 450 °C for 1 h (Figure 9g). This is also confirmed by the thermogram showed in Figure 6c. There is a total weight loss of only 4.7%, and up to 330 °C, the weight loss is almost null. These observations corroborate the mechanical properties obtained for  $\gamma$  alumina samples, high hardness and high density. The pore structure is very strong since it did not break up to 450 °C.

The formation of diaspore is further strong evidence of the retention of water in closed pores, confirming the mechanism for the “cold-sintering” process.<sup>5</sup> Without water in the structure, it is impossible to have the formation of this monohydroxide.

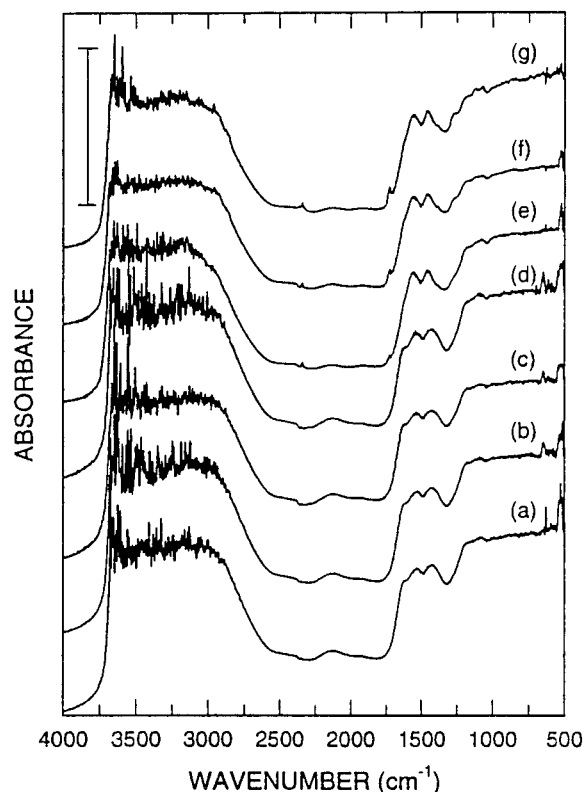


**Figure 9.** FTIR absorption spectra of  $\gamma$ - $\text{Al}_2\text{O}_3$  samples compacted at 4.5 GPa and 562 °C obtained in a vacuum cell after treatment at different temperatures: (a) RT and ambient pressure; (b)–(g) obtained in a vacuum at (b) RT, (c) 100, (d) 200, (e) 300, (f) 400, and (g) 450 °C. The bar value is 2 in absorbance units.

## Conclusions

The effect of thermal treatments at HP (4.5 GPa), from RT up to 800 °C, in  $\gamma$ - $\text{Al}_2\text{O}_3$  nanosize powders was studied. The best samples of  $\gamma$ - $\text{Al}_2\text{O}_3$  were obtained at temperatures between 513 and 565 °C, during only 10 min of HP processing. These samples were dense (95% of theoretical density), very hard (17 GPa), being near to the value of  $\alpha$ - $\text{Al}_2\text{O}_3$  (20 GPa), and transparent. For the first time, nanocrystalline  $\gamma$ - $\text{Al}_2\text{O}_3$  bulk samples were obtained with this set of improved optical and mechanical properties. From temperatures above 565 °C, a sequence of phase transformations produced by this process are observed;  $\gamma$  phase transforms to  $\alpha$  phase and diasporite just above 565 °C. The complete transformation to  $\alpha$  phase only occurs above 755 °C, at a lower temperature than in heat treatments at ambient pressure.

Information about the mechanisms involved in the compaction process at HP, especially with regard to the role of adsorbed water in the system, were obtained using FTIR and TGA techniques. The HP compaction of  $\gamma$ - $\text{Al}_2\text{O}_3$  at RT promotes a reduction of 33% of the adsorbed water content and at the same

time causes the trapping of part of the adsorbed water in closed pores. This structure is formed by a dehydroxylation reaction between bridged OH groups during the HP compaction and can be explained by a “cold-sintering” model, proposed for  $\text{SiO}_2$ .

For the samples processed at HP/HT, the adsorbed water remains trapped in closed pores and is not liberated even after heat treatment in a vacuum at 450 °C, which is a result of the formation of a strong structure. The mechanical and optical properties of the samples confirm this idea, as well as the formation of diasporite. Additionally, it was observed that the water plays an important role in this kind of compaction process, contributing to improving the properties of these samples.

**Acknowledgment.** This research was supported by FAPERGS, CNPq, PADCT, CAPES, and FINEP (Brazil). We would like to thank Dr. João H. Z. dos Santos for the BET measurements (IQ-UFRGS).

## References and Notes

- (1) Mishra, R. S.; Leshner, C. E.; Mukherjee, A. K. *J. Am. Ceram. Soc.* **1996**, 79, 2989.
- (2) Mo, S.; Xu, Y.; Ching, W. *J. Am. Ceram. Soc.* **1997**, 80, 1193.
- (3) Gallas, M. R.; Hockey, B.; Pechenik, A.; Piermarini, G. J. *J. Am. Ceram. Soc.* **1994**, 77, 2107.
- (4) Gallas, M. R.; Rosa, A. R.; Costa, T. M. H.; Jornada, J. A. H. *J. Mater. Res.* **1997**, 12, 764.
- (5) Costa, T. M. H.; Gallas, M. R.; Benvenutti, E. V.; Jornada, J. A. H. *J. Non-Cryst. Sol.* **1997**, 220, 195.
- (6) Wefers K.; Misra, C. *Oxides and Hydroxides of Aluminum*; Alcoa Laboratories, 1987; no. 19.
- (7) Guha, S.; Agahi, F.; Pezheshki, B.; Kash, J. A.; Kisker, D. W.; Bojarkzuk, N. A. *Appl. Phys. Lett.* **1996**, 68, 906.
- (8) Baraton, M. I.; Quintard, P. *J. Mol. Struct.* **1982**, 79, 337.
- (9) Ying, J. Y. *Mechanical Properties and Deformation Behavior of Materials Having Ultra-Fine Microstructure*; Kluwer Academic Publishers: Netherlands, 1993; pp 565–570.
- (10) Knözinger, H.; Ratnasamy, P. *Catal. Rev.—Sci. Eng.* **1978**, 17, 31.
- (11) Peri, J. B.; Hannan, R. B. *J. Phys. Chem.* **1960**, 64, 1526.
- (12) Peri, J. B. *J. Phys. Chem.* **1964**, 69, 211.
- (13) Cocke, D. L.; Johnson, D. E.; Merrill, R. P. *Catal. Rev.—Sci. Eng.* **1984**, 26, 163.
- (14) Dragoo, A. L.; Diamond, J. J. *J. Am. Ceram. Soc.* **1967**, 50, 568.
- (15) Johnston, G. P.; Muenchausen, R.; Smith, D. M.; Fahrenholtz, W.; Foltyn, S. J. *J. Am. Ceram. Soc.* **1992**, 75, 3293.
- (16) Michael, G.; Ferch, H. *Technical Bulletin of Pigments*; Degussa, 1984, no. 19.
- (17) Khvostantsev, L. G. *High Temp. High Pressures* **1984**, 16, 165.
- (18) Chu, C. C. Ph.D. Thesis, University of East Anglia, 1983.
- (19) Ealet, B.; Elyakhloufi, M. H.; Gillet E.; Ricci, M. *Thin Solid Films* **1994**, 250, 92.
- (20) Zecchina, A.; Coluccia, S.; Morterra, C. *Appl. Spectrosc. Rev.* **1985**, 21, 259.
- (21) Michalske, T. A.; Bunker, B. C. *J. Appl. Phys.* **1984**, 56, 2686.
- (22) Ray, S. P. *J. Am. Ceram. Soc.* **1992**, 75, 2605.
- (23) Matsushima, S.; Kennedy, G. C.; Akella, J.; Haygarth, J. *Am. J. Sci.* **1967**, 265, 28.
- (24) Fockenber, T.; Wunder, B.; Grevel, K.-D.; Burchard, M. *Eur. J. Miner.* **1996**, 8, 1293.
- (25) Capponi, J. J.; Chenavas, J.; Joubert, J. C. *Bull. Soc. Fr. Miner. Cristall.* **1972**, 95, 412.
- (26) Chen, W.; Pechenik, A.; Dapkunas, S. J.; Piermarini, G. J.; Malghan, S. G. *J. Am. Ceram. Soc.* **1994**, 77, 1005.